

Characterisation and analysis of the impact of cold jointing in cemented paste backfill stopes

Bre-Anne Sainsbury¹, David Sainsbury², Dean Harty³, Florencio Felipe⁴, Marc Ruest⁵ and David McLoughney⁶

¹ Deakin University, Waurn Ponds, VIC, Australia, breanne.sainsbury@deakin.edu.au

² Geotechnica, Melbourne, VIC, Australia, david.sainsbury@geotechnica.com.au

³ Northern Star Resources, Perth, WA, Australia, DHarty@nsrld.com

⁴ Agnico Eagle Mines Limited, Fosterville, VIC, Australia, Florencio.Felipe@agnicoeagle.com

⁵ Lundin Mining, Vancouver, BC, Canada, marc.ruest@lundinmining.com

⁶ BHP, Adelaide, SA, Australia, david.mcloughney@bhp.com

Abstract

The presence of discontinuities (cold, batch, flow, slick, slurry or water joints) within cemented paste backfill are known to have an impact on the stability of underhand stope exposures. Currently there is limited understanding of the mechanical properties of these internal discontinuities. A geomechanical testing program has been completed that measures the tension response of synthetic discontinuities that have been created in cemented paste backfill in the laboratory. Three-dimensional modelling has been completed to demonstrate the effect on stability from the presence of discontinuities within a CPB fill mass that create backfill beams. It has been shown that when a backfill beam height is greater than 70% of the span width, its presence is unlikely to cause instability issues. As such, it is advised that this value be considered as the minimum thickness of a continuous plug pour to minimise dilution.

Key Words: cold joint; slick joint; slurry joint; strength; cemented paste backfill; backfill beam

Introduction

Placement of cemented paste backfill (CPB) at many underground mines is, in many cases, discontinuous due to interruptions and delays in operational shift schedules, plant batching procedures and maintenance required on the reticulation system. This discontinuous filling can result in the formation of planes of weakness (discontinuities) between CPB pours which are referred to as ‘cold joints’ ‘batch joints’ or ‘flow joints’. The frequency of discontinuities within the fill mass can be further increased during flushing of the reticulation system whereby water or low cement ‘slick’ products are flushed through the pipelines. These joints are sometimes referred to as ‘slurry’, ‘slick’ or ‘water joints’. The typical discontinuous fill profile of a stope that creates backfill beams has previously been documented by Hasan *et al.* (2014) and is presented in Figure 1.

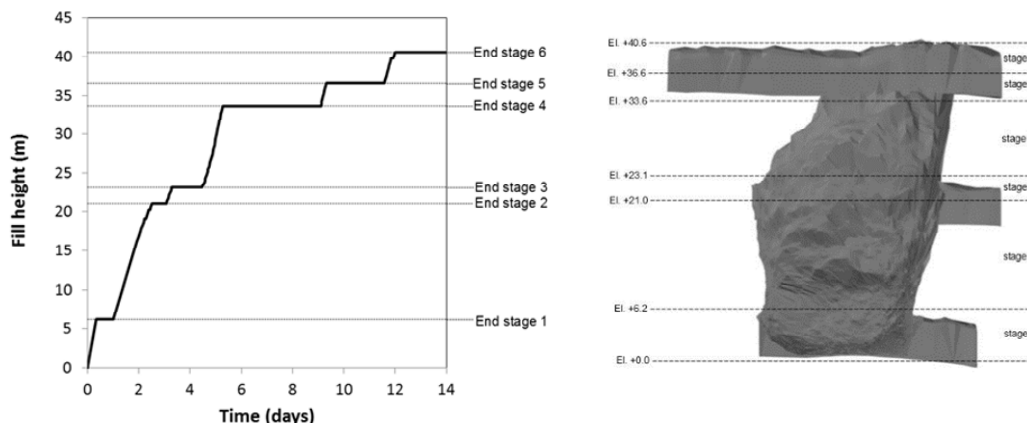


Figure 1. Typical discontinuous filling sequence of a stope (modified after Hasan *et al.*, 2014).

The presence of any of these discontinuities (cold, batch, flow, slick, slurry or water joints) within CPB are known to have an impact on the stability behaviour of underhand stope exposures (Li et al. 2014). They have previously been observed to be a contributor to an underhand backfill failure at the Lucky Friday Mine (Johnson et al. 2015) and dilution at the Henty Mine (Sainsbury and Cai 2001) and Fosterville Gold Mine (Farrington 2020). Although they are frequently observed during exposure (Figure 2) there is limited understanding of their mechanical properties and impact on CPB exposure design (Grabinsky et al. 2022).

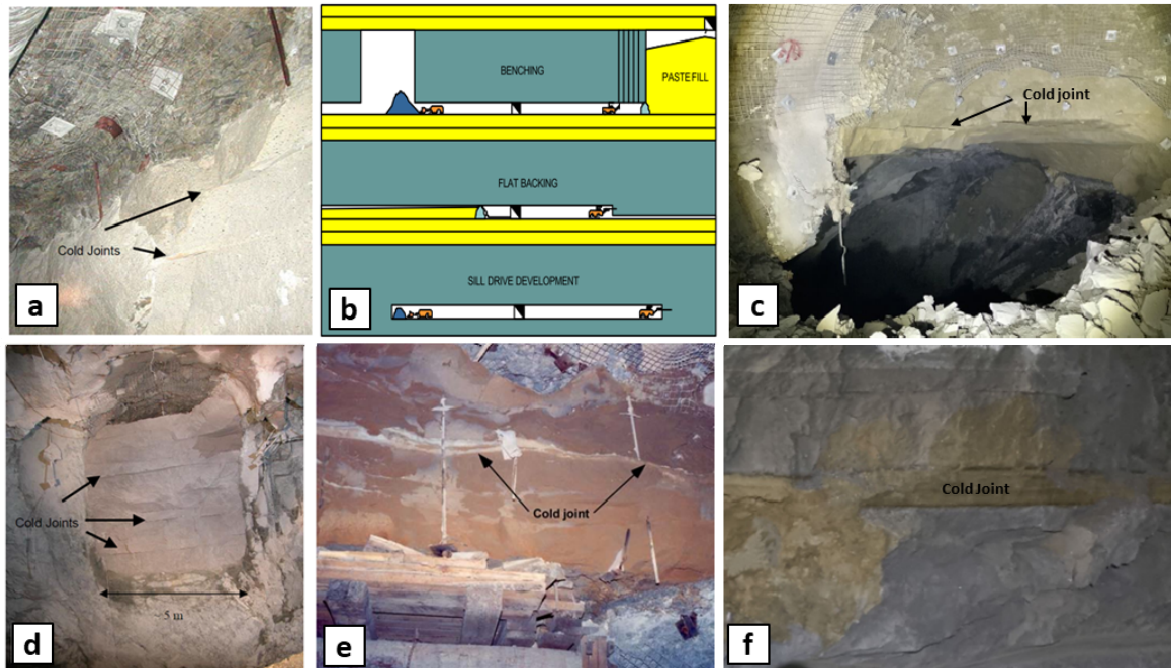


Figure 2. Cold joints observed in paste fill exposures at (a,b) Henty Mine (modified after Sainsbury and Cai 2001) (c) Fosterville Gold Mine (modified after Farrington, 2020) (d) Kanowna Bell Mine (e) Lucky Friday Mine (modified after Johnson et al. 2015) (f) Kibali Mine.

An attempt was made by Johnson *et al.* (2015) to characterise the strength of cold joints at the Lucky Friday Mine. Their results are summarised in Figure 3. Cold joints retrieved from *in situ* samples were characterised with a mean direct tension strength of 0.16 MPa. This value equates to 65% the homogenous direct tension strength and 4% the measured CPB UCS. However, due to limitations associated with sample retrieval and testing, the results were considered inconclusive.

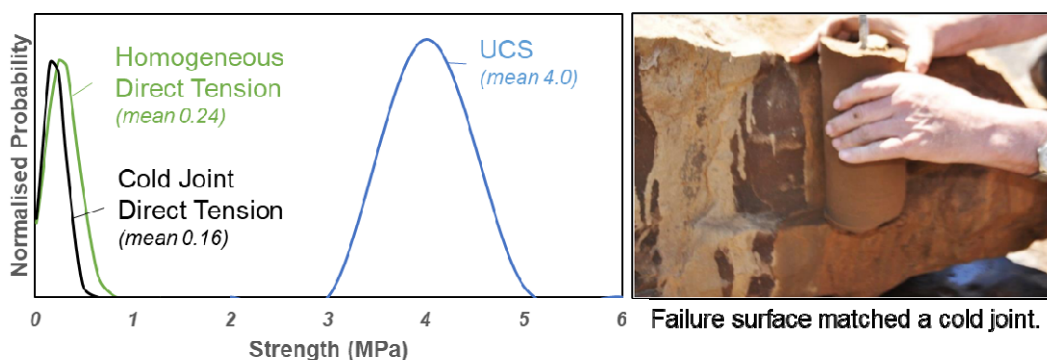


Figure 3. Characterisation of cold joint strength modified after Johnson *et al.* (2015)

Exposure stability modelling that is used to define the required CPB strength and exposure size typically either neglects these internal features (Sainsbury and Urie 2007; Tesarik et al. 2007) or applies conservative tension strength values of 0 kPa tension (Sainsbury and Cai, 2001). In either case, the resulting design may result in dilution (due to an under-estimation of strength required) and/or additional operational costs (increased binder addition) that is not necessary.

To provide some initial guidance on the strength of CPB discontinuities, a geomechanical testing program has been completed that quantifies the tensile response of synthetic discontinuities that have been created in the laboratory. The measured response has been used as direct input to numerical exposure stability analyses that considers their impact on stability and strength requirements for variations in stope spans and backfill beam heights.

Laboratory Testing

CPB samples were prepared in the laboratory in small batches (< 7kg) using mine specific filter cake, binder and water from Northern Star Resources Carouse Dam, Kanowna Belle and Thunderbox Mines; Agnico Eagle's Fosterville Gold Mine (formerly Kirkland Lake Gold) and BHP's Prominent Hill Mine (formerly Oz Minerals). Samples ranged in binder content from 1.5% - 9% and pulp solids from 60% to 85%.

For each batch, the UCS has been determined to provide a control reference for the direct tension responses. For each UCS strength reported in Figure 6 at least 3 samples were used to determine an average reference value. The direct tension response has been established for a range of UCS values based on the direct measurement procedure documented by Sainsbury *et al.*, (2024) that was based on the publications of Alhussainy et al. (2019), Guo et al. (2022) and Pan and Grabinsky (2021). Curing and testing moulds have been printed in a Fortus 450mc Production System with front and back pieces cut from 2 mm Perspex to provide transparency. A bespoke tension bracket has been utilised to strain the sample as presented in Figure 4.

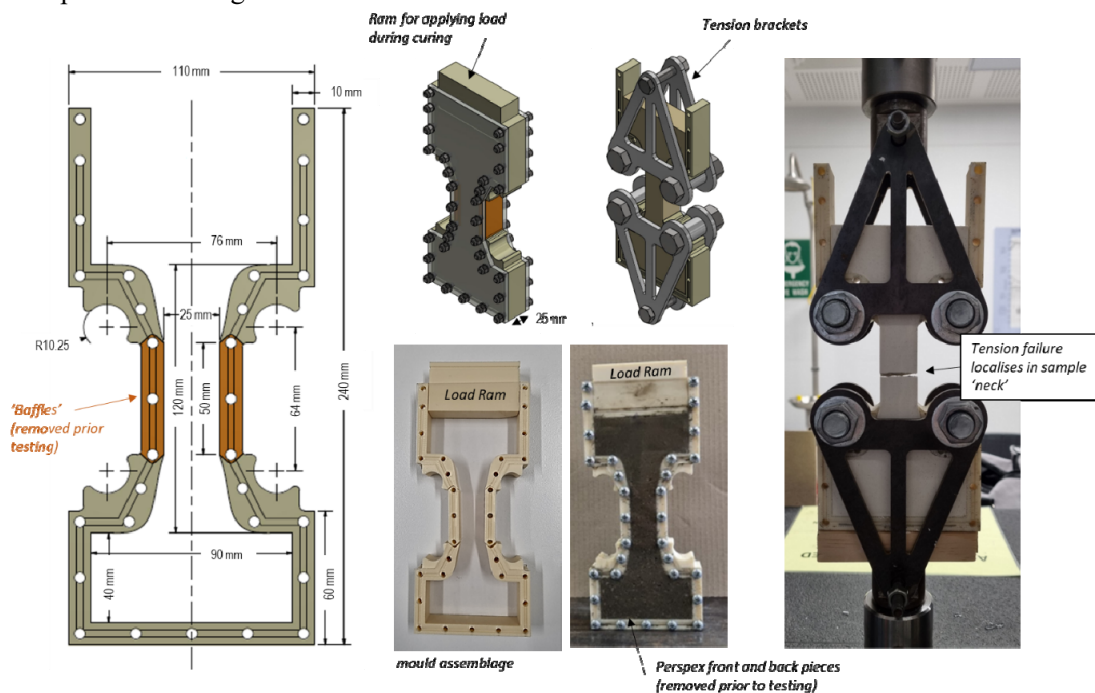


Figure 4. Direct tension mould assemblage and application.

Development of Synthetic CPB Discontinuities

Synthetic CPB discontinuities have previously been generated in the laboratory by Nasir and Fall (2008) and Koupouli et al. (2017). These studies considered the strength of the CPB – rock interface and not internal discontinuities.

For the range of UCS values, direct tension samples were prepared with and without synthetic joints for comparison. In relation to the synthetic joint preparation the following methodology was applied:

- **Cold / Batch joints:** moulds were half filled and cured at 23° and 50% relative humidity for 24 hours. The same batch mix was placed on top of the early age CPB after 24 hours to complete the sample. The samples were cured for 28-days at 23° and 50% relative humidity prior to testing.
- **Water / Slurry / Slick joints:** moulds were half filled. For the water joints, after 10 minutes, 1 mm of room temperature water was placed on top of the paste (to replicate line cleaning). The samples were cured at 23° and 50% relative humidity for 24 hours. After this time, an additional 1 mm of water and the same batch mix was poured to complete the sample to replicate line slicking and continued placement. The samples were cured for 28-days at 23° and 50% relative humidity prior to testing.

Examples of the discontinuous samples after preparation and testing are provided in Figure 5. A summary of the homogeneous results are provided in Sainsbury *et al.*, (2024).

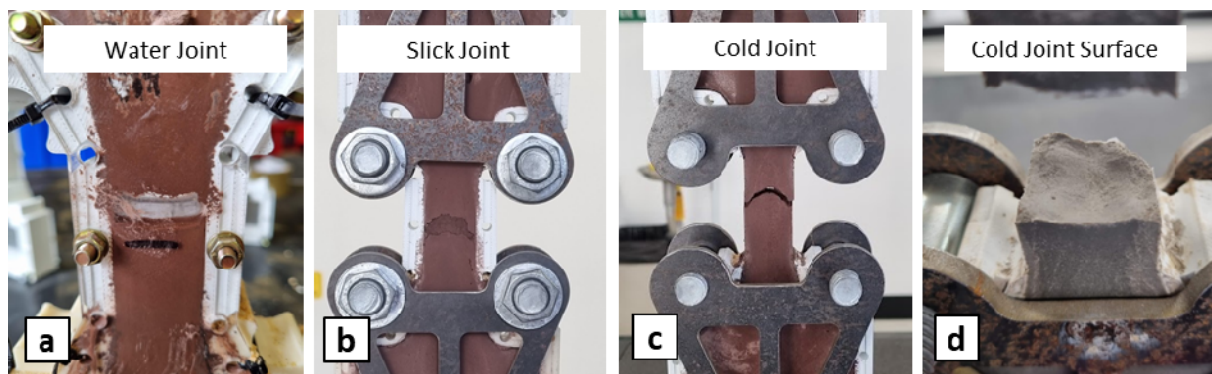


Figure 5. Cemented paste backfill synthetic discontinuities (a) water joint immediately after 'batching' (b) slurry joint after 28-days curing (c) and (d) batch / cold joint after tensile failure

Laboratory Results

A summary of the laboratory test results is provided in Figure 6 that are limited to the UCS strength range 400 kPa - 1600 kPa. This range is typical for mining operations (Brackebusch, 1995) and reflects the significant variability in the range of solids, water and binder content. Significant outcomes of the geomechanical testing include:

- Slick joints are stronger in tension than cold joints and provide a strength of approximately 5.6% of the UCS or 20% the homogenous direct tension response. Consideration of the strength of the measured discontinuity strength at the Lucky Friday Mine (Figure 3) suggests it was a water/slurry/slick joint based on the comparison to its homogenous response.
- Cold joints provide a tension strength of approximately 0.6% of the UCS or 2% of the homogenous direct tension response.

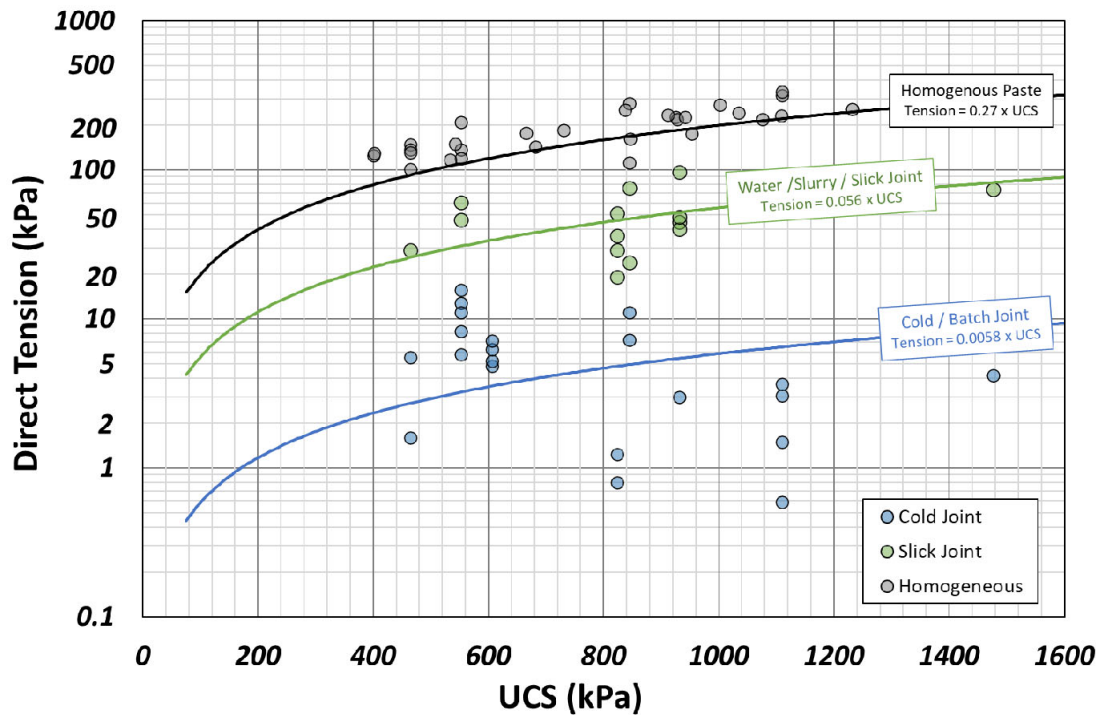


Figure 6. Cemented paste backfills direct tensile strength and consideration of slurry/slick and cold/batch joints.

While relatively small value, the characterisation of some tension strength is more than the conservative estimate of 0 kPa. The impact of these increased strengths on exposure stability modelling results are considered in the following section.

Numerical Analysis

Paste fill exposures created by adjacent mining must be strong enough to prevent failure of the entire fill mass and major sloughing of the vertical and underhand exposure faces. Mitchell (1983, 1991) proposed a series of analytical solutions that for vertical and underhand cemented backfill exposure stability that are still often used, at least for preliminary design, and has motivated subsequent empirical design methods (Pakalnis *et al.*, 2005; Hughes, 2014). Fully employing the Mitchell solutions requires knowledge of the backfill material's UCS, Modulus, and tension strength as well as estimates of stope wall closure. Multiple authors (Oulbacha, 2014; Pagé *et al.*, 2019; Grabinsky, Jafari and Pan, 2022) have demonstrated that these existing approaches have limited applicability, and more generally a full analysis in support of rational design will require numerical modelling that incorporates the effect of the surrounding rock mass and confining stress on the material's stiffness and mobilized strength.

To analyse the performance of paste exposures, a three-dimensional numerical modelling approach has been adopted with the FLAC^{3D} program (Itasca Consulting Group, 2022). The modelling methodology used within this report has been developed and continuously improved over a period of 23 years based on the design, implementation and back-analysis of cemented backfill exposures at operating mines throughout the world as documented in (Sainsbury *et al.*, 2003; Sainsbury and Urie, 2007; Sainsbury and Sainsbury, 2014; and Shiels and Sainsbury, 2020).

Model Conditions

The numerical analysis includes the consideration of a simplified four stope sequence that includes two vertical exposures and one underhand (horizontal) exposure on Stope 1 as presented in Figure 7. For the

simplified mining sequence, a range of stope strike lengths (10, 20 and 30m) and backfill beam heights created by the presence of a cold joint (1, 2, 3 and 7m above the stope floor) have been considered to quantify the UCS required to maintain stability (FOS ~ 1).

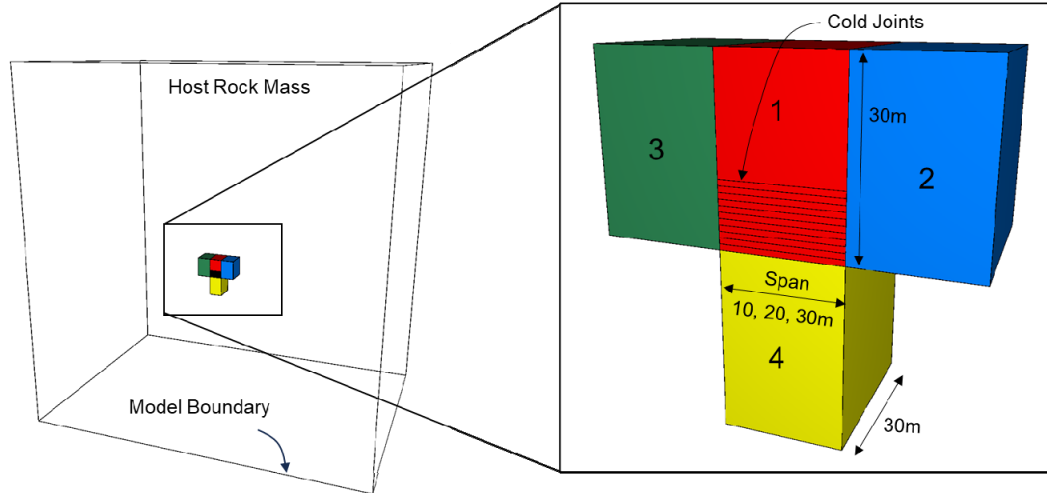


Figure 7. Model geometry and mining sequence including location of cold joints in Stope 1

A lithostatic vertical stress profile with a horizontal stress twice this has been assigned and the stopes have been simulated at a depth of 700m below the ground surface. These stress conditions are representative of the *in situ* conditions at many underground stoping operations.

Material Properties

Wall rock

Due to its strain-softening nature, the stability response of paste backfill is influenced by internal stresses that are controlled by curing age and exposure. It is also influenced by the host rock mass that yields and converges/diverges during the mining sequence that results in stress redistribution and displacements in the backfilled stope (Qi *et al.*, 2022). A smaller CPB span in a more deformable host rock is most exposed to deformations. As such, the representation of the host rock mass in a numerical exposure stability model is critical. The host rock mass has been represented in the simplified model as an elastic medium with properties consistent with UCS 100 GSI 55 and m_i 18.

Paste fill

Density, modulus and tension values for the homogeneous paste fill mass have been derived based on the geomechanical database presented in Sainsbury *et al.* (2024) and the assigned UCS. A friction angle (ϕ) of 30° has been assigned to the CPB which is consistent with geomechanical characterisations completed by Brummer, Andrieux and O'Connor (2003) and Rankine and Sivakugan (2007). Cohesion (c) has been assigned based on ϕ and UCS based on the Mohr-Coulomb Equation 1.

$$UCS = \frac{2c \cos \phi}{1 - \sin \phi} \quad (1)$$

Each stope is filled with sequentially with a 2m lift height with increasing strength and stiffness to accurately simulate the internal stress distribution within each fill mass.

Cold joints

Interfaces that are able to slip and separate have been used to represent cold joints within the numerical model. The explicit representation of the cold joint is critical in being able to accurately capture the

backfill beam bond strength and flexure behaviour that analytical and implicit numerical solutions can not (Sainsbury and Sainsbury, 2017; Hu *et al.*, 2020). Cold joint tension strengths have been determined based on the assigned UCS and direct tension test data presented in Figure 6. A friction angle of 30° has been assigned to the cold joints. This value represents the residual friction angle of CPB materials published by Pan, Grabinsky and Guo (2021). It is also consistent with preliminary direct shear responses observed for cold joints that are presented in Figure 8.

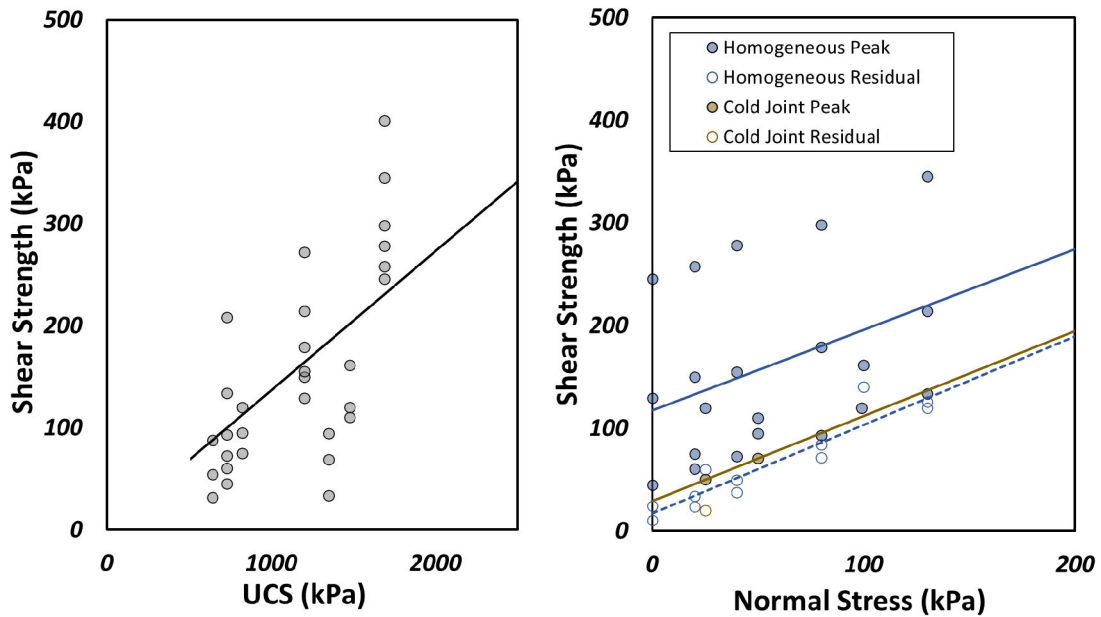


Figure 8. Shear response of paste fill cold joints. Homogenous responses are reported after Pan, Grabinsky and Guo (2021)

Cohesion values for the cold joints have been determined based on the shear (τ) responses (Figure 8 left) generalised in Equation 2.

$$\tau = 0.14(UCS) \quad (2)$$

Normal stresses in the order of 150 – 250 kPa have been measured in an *in situ* stope (Thompson, Bawden and Grabinsky, 2012). Normal stress of 200 kPa has been used to determine the cohesion (c) based on the direct shear results (Figure 8) and traditional Coulomb–Terzaghi shear strength Equation 3.

$$c = 0.0309(UCS) - 10.3e3 \quad (3)$$

Where c and UCS are quantified in Pa.

Normal and shear stiffness values of the cold joint interface have been scaled based on the CPB modulus. Example results for the 20m stope span and 1m cold joint spacing are presented in Figure 9. For these results a FOS of 1 has been inferred at a CPB UCS of 1850 kPa.

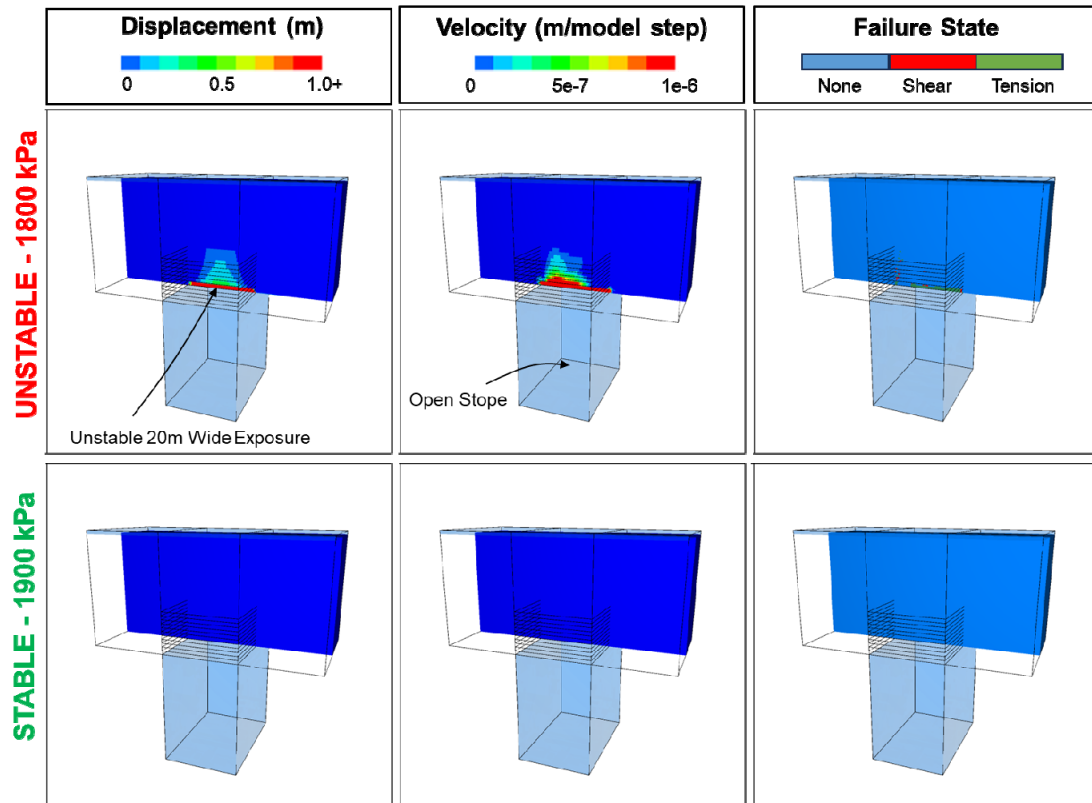


Figure 9. Example model results presented for 20m slope span and 1m beam heights.

A summary of all the simulation results compiled are presented in Figure 10. It is noted here that the results for repetitive cold joint locations (e.g. stacked beams) are the same as those for a single beam since depth of failure has not been considered in the definition of instability for this study. Furthermore, the failure mode may change between simulation sequences since the increase in beam thickness is more likely result in a more complex failure mode that includes a combination of tension, flexure and shear.

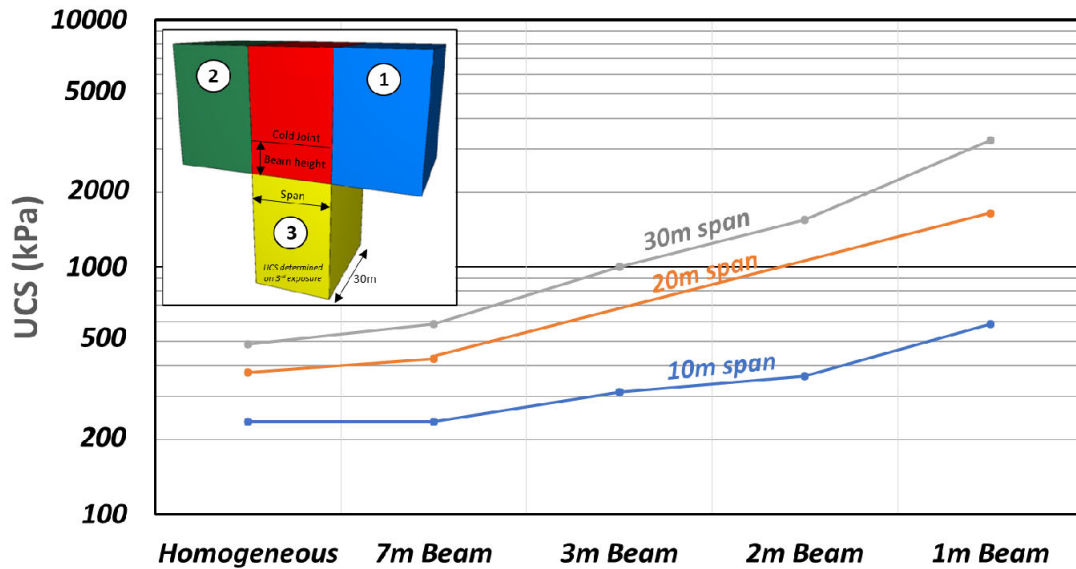


Figure 10. UCS required to maintain FOS 1 on third exposure with decreasing paste fill beam heights created by cold joints.

The results have been normalised in Figure 11 that relates minimum strength required to maintain a FOS of 1 to the relative backfill beam height. The term Strength Factor has been defined that relates the design (homogeneous) strength of the CPB to the strength of the CPB with a cold joint within it. Span relates to the minimum slope dimension in the stope exposure regardless whether it is along or across strike.

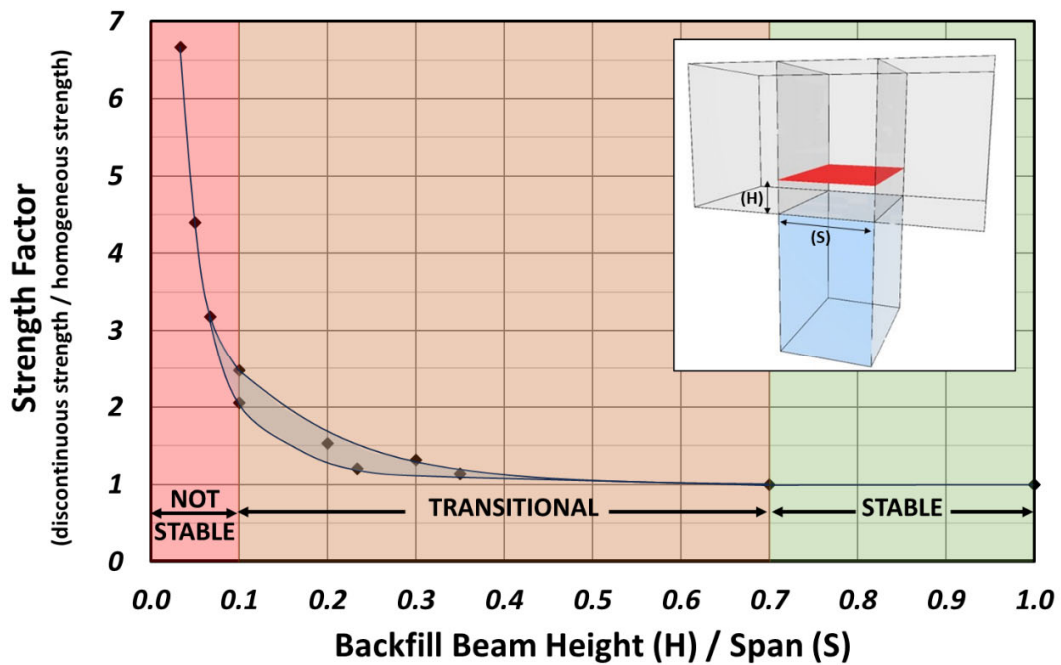


Figure 11. Normalised relationship between paste strength required to maintain FOS 1 and backfill beam height (H) relative to exposed span (S) for third exposure of stope.

Discussion

Typical CPB exposure design includes a FOS of 1.5. This FOS accounts for many factors including variations in batch dosing and variations in ambient curing conditions. When this FOS is applied to the presence of discontinuities formed during placement it is able to account for beam heights that are 0.15 – 0.25 the span width based on Figure 11. The application of Figure 11 can be used to determine the stability of a slope when a discontinuity has been formed or used to determine the minimum height of a plug pour as outlined in the examples below.

Example 1

A cold joint has formed during filling at a height of 4m above the stope floor. The span of the stope on its 3rd exposure is 12m. This provides a $H/S = 0.3$. The strength factor can be determined to be between 1.1 and 1.3. This is below 1.5 and suggest that the stope should still be stable if a FOS of 1.5 has been applied to the strength during design.

Example 2

Based on filling procedures, a cold joint beam height of 4m occurs for all stopes. The planned exposed stope span is 30m. This provides a $H/S = 0.13$. In order to negate the effect of the cold joint the UCS of the CPB should be increased by a factor of 2 (or 200%) to maintain stability and reduce dilution.

It is noted that these examples are provided to indicate how Figure 11 may be used by operational personnel to plan plug pours and/or provide guidance for expected dilution. Figure 11 is provided as an indication of backfill stability and is in no way a suggestion that the strength of paste should be increased by up to 700% in the case of cold joints.

Conclusions

Laboratory testing on the direct tensile response of discontinues in CPB have been conducted. The results suggest that slick joints are stronger in tension than cold joints and provide a strength of approximately 5.6% of the UCS or 20% the homogenous direct tension response. Cold joints provide a tension strength of approximately 0.6% of the UCS or 2% of the homogenous direct tension response.

The strength responses have been simulated in numerical exposure stability analysis for which the results have been generalised and are presented in a design chart. Based on the generalised results the following conclusions can be made:

- When a backfill beam height is greater than 70% of the span width, its presence is unlikely to cause instability issues. As such, it is advised that this value be considered as the minimum thickness of a continuous plug pour to minimise dilution.
- Significant instability is observed when backfill beam heights are less than 10% the stope span.

Acknowledgements

This research has been funded by Northern Star Resources Carouse Dam, Kanowna Belle and Thunderbox Mines; Agnico Eagle Fosterville Gold Mine (formerly Kirkland Lake Gold); BHP Prominent Hill (formerly Oz Minerals); Lundin Mining and Geotechnica.

Many thanks also to the Honors students at Deakin University who have contributed to the testing of cemented paste backfill who include Josh Phelan, Jordan Jones, Ahmad Albaba, Alex Hyland, Hamza Waqar, Rana Saim Ashraf, Abdul Rafay Imran, Maaz Salman, Shui (James) Chen and Nathan Marley.

References

Alhussainy, F. et al. (2019) 'A new method for direct tensile testing of concrete', Journal of Testing and Evaluation, 47(2). Available at: <https://doi.org/10.1520/JTE20170067>.

- Brackebusch, F. (1995) 'Basics of paste backfill systems', *International Journal of Rock Mechanics and Mining Sciences and Geomechanics Abstracts*, 32(3), p. 122A.
- Brummer, R., Andrieux, P. and O'Connor, C. (2003) 'Stability Analyses of Undermined Sill Mats for Base Metal Mining', in B. et Al (ed.) *Proceedings of the 3rd FLAC and Numerical Modelling in Geomechanics*. Sudbury: A.A. Balkema, pp. 189–195.
- Farrington, M. (2020) 'Personal Communication'. Fosterville, Victoria, Australia: Fosterville Gold Mine.
- Grabinsky, M., Jafari, M. and Pan, A. (2022) 'Cemented Paste Backfill (CPB) Material Properties for Undercut Analysis', *Mining*, 2(1), pp. 103–122. Available at: <https://doi.org/10.3390/mining2010007>.
- Guo, L. et al. (2022) 'Experimental Study on Direct Tensile Properties of Cemented Paste Backfill', *Frontiers in Materials*, 9(March), pp. 1–10. Available at: <https://doi.org/10.3389/fmats.2022.864264>.
- Hasan, A. et al. (2014) 'In situ measurements of cemented paste backfilling in an operating stope at Lanfranchi Mine', in Y Potvin & AG Grice (ed.) *MineFill 2014 : Proceeding of the 11th International Symposium on Mining with Backfill*. Perth: Australian Centre for Geomechanics, pp. 327–336. Available at: https://doi.org/10.36487/acg_rep/1404_26_hasan.
- Hu, C. et al. (2020) 'Physical investigation on the behaviours of voussoir beams', *Journal of Rock Mechanics and Geotechnical Engineering*, 12(3), pp. 516–527. Available at: <https://doi.org/10.1016/j.jrmge.2019.12.007>.
- Hughes, P.B. (2014) *Design Guidelines: Underhand Cut and Fill Cemented Paste Backfill Sill Beams*. University of British Columbia.
- Itasca Consulting Group (2022) 'FLAC3D 7.0 Explicit Continuum Modeling of Non-Linear Material Behavior in 3D'. Minneapolis: Itasca Consulting Group.
- Johnson, J.C. et al. (2015) 'Strength and elastic properties of paste backfill at the Lucky Friday Mine, Mullan, Idaho', 49th US Rock Mechanics / Geomechanics Symposium 2015, 3, pp. 2321–2332.
- Koupouli, N., Belem, T. and Rivard, P. (2017) 'Shear strength between cemented paste backfill and natural rock surface replicas', in M. Hudyma and Y. Potvin (eds) *Underground Mining Technology 2017*. Perth: Australian Centre for Geomechanics, p. 375. Available at: https://papers.acg.uwa.edu.au/p/1710_29_Koupouli/.
- Mitchell (1983) *Earth Structures Engineering*. Springer Dordrecht. Available at: <https://doi.org/DOI> <https://doi.org/ezproxy-f.deakin.edu.au/10.1007/978-94-011-6001-8>.
- Mitchell, R.J. (1991) 'Sill mat evaluation using centrifuge models', *Mining Science and Technology*, 13(3), pp. 301–313. Available at: [https://doi.org/10.1016/0167-9031\(91\)90542-K](https://doi.org/10.1016/0167-9031(91)90542-K).
- Nasir, O. and Fall, M. (2008) 'Shear behaviour of cemented pastefill-rock interfaces', *Engineering Geology*, 101(3–4), pp. 146–153. Available at: <https://doi.org/10.1016/j.enggeo.2008.04.010>.
- Oulbacha, Z. (2014) *Analyse numérique de la stabilité des piliers-dalles en remblai cimenté: une vérification des modèles de Mitchell*. Ecole Polytechnique de Montreal. Available at: <https://doi.org/10.13140/RG.2.2.15670.78408>.
- Pagé, P. et al. (2019) 'Numerical investigation of the stability of a base-exposed sill mat made of cemented backfill', *International Journal of Rock Mechanics and Mining Sciences*, 114(January), pp. 195–207. Available at: <https://doi.org/10.1016/j.ijrmms.2018.10.008>.
- Pakalnis, R. et al. (2005) 'Design spans-underhand cut and fill mining', in *Proceedings of 107th CIM-AGM Toronto*.
- Pan, A.N. and Grabinsky, M.W.F. (2021) 'Tensile strength of cemented paste backfill', *Geotechnical Testing Journal*, 44(6), pp. 1886–1897. Available at: <https://doi.org/10.1520/GTJ20200206>.
- Pan, A.N., Grabinsky, M.W.F. and Guo, L. (2021) 'Shear Properties of Cemented Paste Backfill under Low Confining Stress', *Advances in Civil Engineering*, 2021. Available at: <https://doi.org/10.1155/2021/7561977>.
- Qi, C. et al. (2022) 'Stability Evaluation of Layered Backfill Considering Filling', *Minerals*, 12(271). Available at: <https://doi.org/https://doi.org/10.3390/min12020271>.
- Rankine, R.M. and Sivakugan, N. (2007) 'Geotechnical properties of cemented paste backfill from Cannington Mine, Australia', *Geotechnical and Geological Engineering*, 25(4), pp. 383–393. Available at: <https://doi.org/10.1007/s10706-006-9104-5>.
- Sainsbury, B. et al. (2024) 'Characterisation of the geomechanical properties of cemented paste backfill for design', in A. Fourie and D. Reid (eds) *Proceedings of Pastefill 2024*. Melbourne: Australian Centre for Geomechanics, Perth.
- Sainsbury, B.L.L. and Sainsbury, D.P.P. (2017) 'Practical Use of the Ubiquitous-Joint Constitutive Model for the Simulation of Anisotropic Rock Masses', *Rock Mechanics and Rock Engineering*, 50(6), pp. 1507–1528. Available at: <https://doi.org/10.1007/s00603-017-1177-3>.

- Sainsbury, D. and Sainsbury, B. (2014) 'Design and implementation of cemented rockfill at the Ballarat Gold Project', Mine Fill 2014 Proceeding of the 11th International Symposium on Mining with Backfill, pp. 1–12.
- Sainsbury, D.P. et al. (2003) 'Investigation of the geomechanical criteria for safe and efficient crown pillar extraction beneath stabilised rockfill at the Crusader Mine', 10th ISRM Congress, pp. 1001–1006.
- Sainsbury, D.P. and Cai, Y. (2001) 'Numerical analysis of crown pillar recovery techniques beneath paste fill', *FLAC and Numerical Modeling in Geomechanics*, pp. 295–301. Available at: <https://doi.org/10.1201/9781003077527-44>.
- Sainsbury, D.P. and Urie, R. (2007) 'Stability Analysis of Horizontal and Vertical Paste Fill Exposures at the Raleigh Mine', in *MINEFILL 2007 : Proceedings of the International Symposium on Mining with Backfill*. Montreal, Quebec, CIM.
- Shiels, A. and Sainsbury, D. (2020) 'Crown pillar extraction with paste underhand stoping', in *Underground Mining Technology 2020 : Proceedings of the Second International Conference on Underground Mining Technology*. Australian Centre for Geomechanics, Perth, pp. 217–230. Available at: https://doi.org/10.36487/acg_repo/2035_08.
- Tesarik, D.R. et al. (2007) *Numeric model of a cemented rockfill span test at the Turquoise Ridge Mine, Golconda, Nevada, USA*.
- Thompson, B.D.B., Bawden, W.F. and Grabinsky, M.W. (2012) 'In situ measurements of cemented paste backfill at the Cayeli mine', *Canadian Geotechnical Journal*, 49(7), pp. 755–772. Available at: <https://doi.org/10.1139/T2012-040>.

Acronyms

CPB	Cemented Paste Backfill
FOS	Factor of Safety
GSI	Geological Strength Index
UCS	Unconfined Compressive Strength